Investigation of the Dielectric β-Process in Polyisobutylene by Incoherent Quasielastic Neutron Scattering

A. Arbe and J. Colmenero*

Departamento de Física de Materiales, Universidad del País Vasco, Apartado 1072, 20080 San Sebastián, Spain

B. Frick

Institut Laue-Langevin, 156X, 38042 Grenoble CEDEX, France

M. Monkenbusch and D. Richter

Institut für Festkörperforschung, Forschungszentrum Jülich, 52425 Jülich, Germany

Received December 8, 1997; Revised Manuscript Received May 5, 1998

ABSTRACT: Recently by dielectric spectroscopy a new secondary relaxation process in polyisobutylene (PIB) was detected showing all the signatures of a Johari−Goldstein relaxation [Richter, D; Arbe, A.; Colmenero, J.; Monkenbusch, M.; Farago, B.; Faust, R. *Macromolecules* **1998**, *31*, 1133]. Using high resolution neutron backscattering, we investigated the quasielastic neutron spectra from protonated PIB which are related to this process as a function of momentum transfer and temperature. In addition we studied the elastically scattered intensity over a wide temperature range. After multiple scattering corrections all results can be described consistently in terms of a local jump process with the distribution parameters from the dielectric β-relaxation. The spatial extent of the associated protonic motion was determined to be $d = 2.7$ Å. A comparison with the existing body of data for PIB leads to the conclusion that the dielectric β-process and the earlier found δ-process must be identical, thereby revising the assignment of the δ-process as due to methyl group rotation. Finally, we remark on aspects of the relation between quasielastic coherent and incoherent scattering and address the seemingly contradictory result of different length scales revealed for the same process with the two techniques.

I. Introduction

The viscoelastic properties of polyisobutylene (PIB) have been investigated continuously over the last 50 years, rendering it one of the best studied polymers.[1−14] PIB exhibits an α-process which has been thoroughly explored by Ferry et al., who established a shift factor which approaching the glass transition exhibits a relatively weak temperature dependence and thereby qualifies PIB as the least fragile polymer ($\tau_\alpha = \tau_o \exp[DT_o/(T - T_o)]$ with the fragility index $D = 49$ and the Vogel−Fulcher temperature $T_o = 89.2$ K).[1] Later experiments applying spectroscopic techniques such as NMR and ESR did not reproduce the rheologically based temperature dependence but rather indicated a more fragile behavior.[6,11,12] Very recently, however, neutron spin−echo (NSE) experiments were undertaken at the momentum transfer of the first structure factor peak, thereby studying the polymer motion at interchain distances.[15] There, the dynamic response is selective for the relative motion of different chains and reveals the α-relaxation. These NSE experiments demonstrated that at length scales corresponding to the distance between adjacent chains the neutron spectra superimpose with the shift factors from viscous flow, thereby supporting strongly the original findings of Ferry et al. Obviously, the spectroscopic results, which are also reflecting microscopic motions, are not process selective.

Probably as a consequence of the very weak electric dipole moment of the PIB chain, the experimental picture for the secondary relaxations is much less clear. Some time ago Törmälä[6] compiled experimental and theoretical results for PIB: Theoretically, two relaxation processes γ and γ' are predicted.[14] Experimentally by NMR[11,13] and ESR[6] a so-called δ-process was observed which was interpreted as rotations of CH_3 groups. Very recently, by dielectric spectroscopy,[15] we were able to find and characterize a secondary relaxation in PIB which has all the signatures of a Johari−Goldstein β-process.[16] The distribution of jump times τ_β can be well described by a log-normal distribution

$$g_\beta(\ln \tau_\beta) = \frac{k_B T}{\sqrt{\pi}\sigma} \exp\left\{-\left[\frac{k_B T \ln(\tau_\beta/\tau_o^{\beta}) - E_o}{\sigma}\right]^2\right\} \quad (1)$$

with a temperature-dependent width

$$\sigma = 130 - 0.29T \text{ [meV]} \quad (2)$$

where T denotes the temperature in Kelvin, $\tau_o^{\beta} = 1.5 \times 10^{-13}$ s, the average activation energy amounts to $E_o = 260$ meV and k_B is the Boltzmann constant.

Both the temperature dependence as well as the time scale of this process disagree significantly with the earlier theoretical speculations. Some traces of it could also be identified in the dynamic structure factor of PIB at large momentum transfers. Apparently the process had to be associated with a short jump distance.

The aim of the present study was to find and to characterize this dielectric β-process by incoherent quasielastic neutron scattering (IQENS). IQENS accesses the self-correlation function of the moving protons on the appropriate atomic length and time scales, thereby facilitating molecular space−time observations.[17] The experiments were carried out with the goal to explore the length scale of the β-process, to identify

S0024-9297(97)01781-6 CCC: $15.00
Published on Web 07/10/1998

the corresponding time scale, and to compare these results with the dielectric results. Such a comparison is by no means trivial. We note that for polybutadiene discrepancies in the time scale between the relaxation of density fluctuations as observed with coherent neutron scattering and the dipole relaxation both originating from the same β-process by 2 orders of magnitude have been reported.[18,19]

The manuscript is structured as follows: In section II we undertake some theoretical considerations on the self-correlation function and the related incoherent scattering function for a localized jump process as it is assumed for the β-relaxation. Furthermore, we discuss the elastic incoherent structure factor and its measurement by a so-called elastic window scan. Section III contains information on the sample and the experimental conditions. Section IV is devoted to the experimental strategy, the presentation of the results, and the data evaluation. In section V we discuss the results, and in section VI the paper is summarized.

II. Theoretical Considerations on the Incoherent Scattering Function

As a consequence of the largely different cross sections for neutron−proton singlet and triplet states, neutron scattering from proton containing materials is predominantly incoherent, i.e., neutron waves scattered from different protons do not interfere and as consequence the cross section carries information on the self-correlation function of the protons. The double differential neutron cross section $\partial^2/\partial\underline{\Omega}\partial\omega$ is written as

$$\frac{\partial^2\sigma}{\partial\underline{\Omega}\partial\omega} = \frac{k_f}{k_i}\sigma_{inc}^{H} S_{inc}(\underline{Q},\omega) \tag{3}$$

where $\underline{k}_i$ and $\underline{k}_j$ are the incident and scattered neutron wave vectors, $\underline{Q} = \underline{k}_i - \underline{k}_f$ is the momentum transfer, $\hbar\omega = (\hbar^2 k_i^2/2m) - (\hbar^2 k_f^2/2m)$ (m: neutron mass; $\hbar$: Planck constant) is the energy transfer during scattering, and $\sigma_{inc}^{H} = 80.26$ barns is the incoherent cross section of hydrogen. The incoherent scattering function $S_{inc}(\underline{Q},\omega)$ relates to the self-correlation function $G_s(\underline{r},t)$ by double Fourier transformation

$$S_{inc}(\underline{Q},\omega) = \frac{1}{2\pi}\int d\omega\, e^{-i\omega t}\int e^{i\underline{Q}\underline{r}}\, G_s(\underline{r},t)\, d^3r \tag{4}$$

Generally, the β-process is considered as a local jump process with a jump rate

$$\tau_\beta(E)^{-1} = \frac{1}{\tau_o^{\beta}}\exp\left(-\frac{E}{k_B T}\right) \tag{5}$$

which is subject to broad distribution of activation energies. The assumption of a Gaussian distribution of barriers leads to the log-normal distribution of eq 1. Apart from the Debye−Waller factor the isotropically averaged incoherent scattering function for two site jumps has the form

$$S_{inc}(Q,\omega)_{\tau(E)} = \frac{1}{2}\left(1 + \frac{\sin Qd}{Qd}\right)\delta(\omega) + \frac{1}{2}\left(1 - \frac{\sin Qd}{Qd}\right)\frac{1}{\pi}\frac{2/\tau(E)}{\left(\frac{2}{\tau(E)}\right)^2 + \omega^2} \tag{6}$$

where d is the jump distance and $\delta(\omega)$ is a δ-function. We neglect a possible correlation between the jump distance and activation energy. Then the incoherent scattering function for the β-process is obtained by averaging eq 6 with the distribution function of eq 1

$$S_{inc}^{\beta}(Q,\omega) = \int_{-\infty}^{\infty} g_\beta(\ln\tau_\beta) S_{inc}(Q,\omega)_{\tau_\beta(E)}\, d(\ln\tau_\beta) \tag{7}$$

At higher temperatures, when the α-process approaches the β-relaxation, the contribution of the diffusive α-process also has to be considered. Though for our experiments the α-process has only a minor influence, we still include its effect. We follow earlier experience and use the successful concept of statistically independent α- and β-processes and a spatially homogeneous dynamics.[19] With both processes taking place simultaneously, the joint self-correlation function is obtained from a spatial convolution of the corresponding correlation functions for the two processes. In Fourier space this translates into a product of the intermediate scattering functions and into a convolution in ω-space

$$S_{inc}^{\alpha\beta}(Q,\omega) = \int_{-\infty}^{+\infty} S_{inc}^{\alpha}(Q,\omega') S_{inc}^{\beta}(Q,\omega-\omega')\, d\omega' \tag{8}$$

For the α-process we use a Fourier transformed (FT) Kohlrausch−Williams−Watts stretched exponential function with a stretching exponent $\beta = 0.55$ as found by NSE[15] and a Gaussian approximation for the Q-dependence of the characteristic relaxation of the α-process,[20,21] $\tau_{KWW} \propto Q^{-2/\beta}$, leading to

$$S_{inc}^{\alpha}(Q,\omega) = FT\left(\exp\left\{-\left[\frac{t}{\tau_{KWW}(Q,T)}\right]^{\beta}\right\}\right) \tag{9}$$

The self-correlation function of a spatially limited process does not decay to zero for long times but reflects the asymptotic spatial distribution of the moving atom. The Fourier transform of this asymptotic particle distribution is called the elastic incoherent structure factor (EISF) and appears as an elastic contribution in the scattering function. The EISF can thus be considered as the result of the diffraction of a neutron on the long time distribution of an average proton. For the case of a two-site jump process the EISF is particularly simple and is represented by the δ-function contribution in eq 6. The EISF contains all information on the spatial extent of motion.

In a neutron scattering experiment the EISF is measured through the elastic band-pass of a given instrument. Thereby the elastic intensity $I_{el}(Q,\omega \approx 0)$ transmitted by the instrument through the elastic window set by the instrumental resolution function $\mathrm{Res}(\omega)$ is counted:

$$I_{el}(Q,\omega \approx 0) = \int_{-\infty}^{+\infty} S(Q,\omega)\,\mathrm{Res}(\omega)\, d\omega \tag{10}$$

Since the instrumental resolution function has a finite width and for the β-relaxation we deal with a broad distribution of relaxation times, parts of the quasielastic Lorentzian functions which lie in this resolution window also contribute to $I_{el}(Q,\omega \approx 0)$. For the scattering function of eq 6 this leads to

$$I_{el}(Q,\omega \approx 0) = \frac{1}{2}(1 + A) + \frac{1}{2}(1 - A)\frac{\sin Qd}{Qd} \tag{11}$$

Again we have omitted the Debye−Waller factor. The constant A contains the contribution of the different

Lorentzians within the resolution window. Now we describe the resolution function by a Gaussian

$$\mathrm{Res}(\omega) = \frac{\sqrt{\ln 2}}{\sqrt{\pi}\,\omega_{1/2}} \exp\left(-\frac{\omega^2 \ln 2}{{\omega_{1/2}}^2}\right) \qquad (12)$$

where $\omega_{1/2}$ is the half width at half-maximum—an assumption which is well fulfilled in our experiment. Then, with eqs 6 and 7 in the regime of negligible contribution of the α−process we get

$$A = \frac{k_B T}{\sigma\sqrt{\pi}} \int \exp\left[-\left(\frac{k_B T \ln(\tau/\tau_o^{\beta}) - E_0}{\sigma}\right)^2\right] \times \mathrm{erfc}\left(\frac{2\sqrt{\ln 2}}{\tau\omega_{1/2}}\right) \exp\left(-\frac{4 \ln 2}{\tau^2 {\omega_{1/2}}^2}\right) \mathrm{d}(\ln \tau) \quad (13)$$

With the dielectric parameters for the distribution function, knowledge of the Debye−Waller factor and the resolution parameters of the neutron instrument, eq 13 in connection with eq 11, allows a determination of the jump distance d from an elastic experiment alone.

III. Experimental Section

III.1. Sample. The PIB material was purchased from the America Polymer Standard Corp. (Mentor, OH). It has been synthesized by cationic polymerization and was characterized by various techniques. From GPC a molecular weight of M_W = 24900 was inferred agreeing well with light scattering data, revealing M_W = 24200. The number average molecular weight was obtained from vapor pressure osmometry yielding M_N = 19600. The resulting value for M_W/M_N = 1.23 agrees well with what can be deduced from GPC (M_W/M_N = 1.21). The GPC trace shows a tail toward lower molecular weights with the 1% level reached at a molecular weight of about 7000. The sample was filled into flat Al-containers with a nominal thickness of d = 0.015 cm. The resulting neutron transmission at a wavelength *of* λ = 6.2 Å was measured to be 0.925.

II.2. Backscattering Experiment. The quasielastic high-resolution neutron backscattering experiments were performed at the instrument IN16 of the Institute Laue Langevin (ILL) in Grenoble, France. In a backscattering experiment, perfect Si crystals are used as the monochromator and analyzers, and the instrumental resolution is optimized by using backscattering geometry both at the monochromator and the analyzer. The energy variation is performed by moving the monochromator and exploiting the Doppler effect.[22] The energy window of the experiment was set to $\Delta E = \pm 11$ meV at an energy resolution of $\omega_{1/2}$ = 0.49 μeV (half width at half-maximum). The resolution function can be well described by a Gaussian making the instrument sensitive to small quasielastic wings close to the elastic line. The experiment covered a Q-range 0.19 Å$^{-1} \le Q \le$ 1.90 Å^{-1}. The data were grouped to have 12 different Q-values (Q = 0.19, 0.29, 0.32, 0.43, 0.54, 0.65, 0.76, 1.01, 1.29, 1.53, 1.70 and 1.85 Å^{-1}). The flat-shaped sample was positioned perpendicular to the beam. Three temperatures, 260, 270, and 280 K, were studied. The experimental resolution function was obtained from a measurement at 2 K, where the scattering of the sample within the observation window of the instrument is entirely elastic. Background corrections were performed for the scattering of the empty cell, which was subtracted with the proper transmission factor.

In addition to the measurements of the quasielastic spectra the elastic intensity scattered from the sample was studied as a function of temperature covering a temperature range 2 ≤ T ≤ 300 K. With an identical set up of the analyzers as above the intensity $I_{el}(Q,\omega \approx 0)$ was recorded with the Doppler drive at rest. These data were normalized by an extended run at 2 K. Intensities were registered every 2 K (the temperature scan rate was 0.35 K/min).

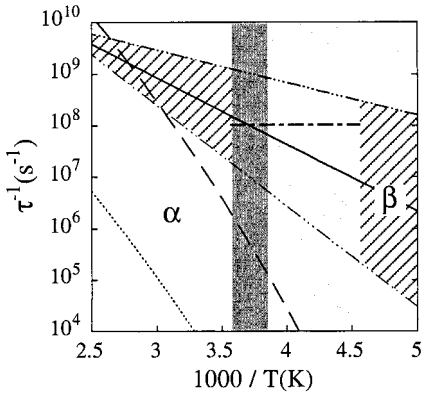

Figure 1. Temperature dependence of the relaxation rates for the α- and β-relaxations: for the different Q values investigated $\tau_{KWW}^{-1}(Q,T)$ lies between the dashed (− −) (τ_{KWW}^{-1} Q = 1.85 Å^{-1},T) and the dotted (···) (τ_{KWW}^{-1} Q = 0, 19 Å^{-1},T) lines. The distribution of relaxation rates for the β−process (average shown by continuous line, corresponding to the activation energy E_o) is located in the crosshatched area between the dashed−dotted lines (−···−), which correspond to activation energies $E_o + \sigma$ (lower line) and $E_o - \sigma$ (upper line). The shaded areas show the temperature ranges of investigation of the quasielastic scattering (dark area) and the elastic intensity (light area). Horizontal dashed−dotted line schematically indicates the IN16 resolution.

Finally for the data evaluation a knowledge of the Debye−Waller factor is important. In the low-temperature regime, where no inelastic broadening occurs within the energy window of IN16, it may directly be read off from the elastic window scan. For the mean square displacement $\langle u^2\rangle$ entering the Debye−Waller factor, exp (− $\langle u^2\rangle$ Q^2/3), we find

$$\langle u^2\rangle = 6.3 \times 10^{-4} T\ [\text{Å}^2] \quad (T < 135\ \text{K}) \qquad (14)$$

relative to the zero point motion contributing to the reference measurement at 2 K. At higher temperatures a direct evaluation of $\langle u^2\rangle$ from the backscattering data alone is not possible, because intensity loss due to the faster components of the jump time distributions occurs, which affects the measured intensity in the elastic window. In this temperature regime we used a combination of extrapolated low-temperature backscattering results and recent spin−echo amplitudes to arrive at the Debye−Waller factor.[15] Here we found

$$\langle u^2\rangle = -0.31 + 2.5 \times 10^{-3} T\ [\text{Å}^2] \quad (160\ \text{K} < T < 390\ \text{K}) \qquad (15)$$

IV. Experimental Results and Data Evaluation

IV.1. Experimental Strategy. The goal of the experiment was to characterize the dielectric β-relaxation by IQENS, an experimental method with space−time sensitivity. Thus, it was important to identify a temperature regime where the β-process falls into the observation window of IN16 and where at the same time the α-process is still slow enough in order not to cause a major quasielastic broadening. Figure 1 shows a relaxation map presenting the temperature-dependent average relaxation rate of the β-process together with the dispersion zone of the α-relaxation. For its evaluation we relate to recent neutron spin−echo results on the α-process.[15] There the following relation for the Kohlrausch−Williams−Watts α-relaxation time τ_{KWW} was found

$$\tau_{KWW} = 4.79 \times 10^{-7} \left(\frac{Q}{Q_o}\right)^{-1.9/\beta} \exp\left(\frac{4370}{T - 89.2}\right) [\text{ns}] \quad (16)$$

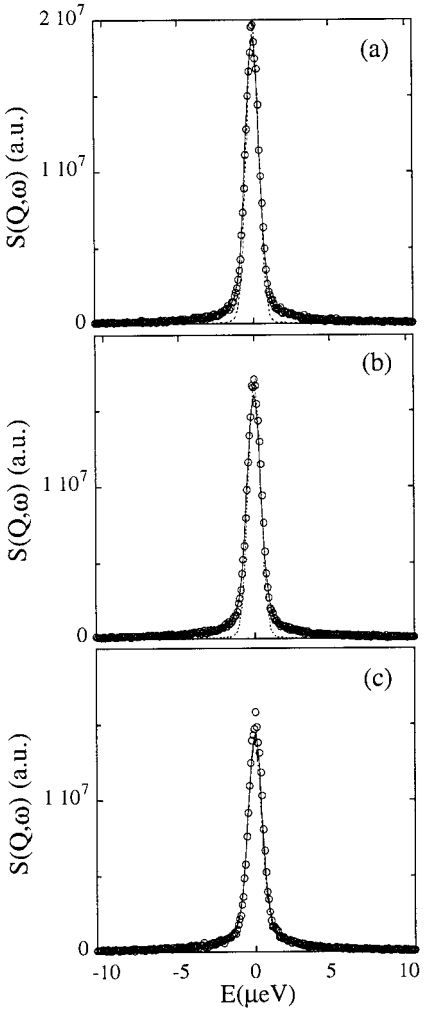

Figure 2. IN16 quasielastic spectra measured at $Q = 1.70$ Å^{-1} and 260 (a), 270 (b), and 280 K (c). Solid lines are the fit results. Dashed lines show the resolution function (2 K spectrum) in parts a and b and the fit when the contribution of the α-relaxation is not taken into account in part c.

where $Q_0 = 1$ Å^{-1}. Figure 1 presents the dispersion zone for the experimental Q range ($0.19 \leq Q \leq 1.85$ Å^{-1}) presenting the relaxation rate $1/\tau_{KWW}$. The shaded area displays the experimental temperature range of our experiment. It selects a region where the β-process is fast enough to be seen, but the α-process is still slow. Since we have to deal with jump time distributions and stretched exponential relaxations in particular at the high-temperature side, some cross talk between both processes cannot be avoided.

IV.2. Experimental Results. Figure 2 presents spectra taken at $Q = 1.70$ Å^{-1} for the three temperatures investigated. At 260 and 270 K (parts a and b of Figure 2, respectively) the data are compared with the instrumental resolution function, and a clear quasielastic foot evolves which is superimposed on a strong elastic peak. Qualitatively this agrees with what is expected for a local relaxation process giving rise to a quasielastic line plus a δ-function contribution from the EISF. At 270 K the quasielastic foot becomes more important and at 280 K finally some influence of the incoming α-relaxation is visible. There the dashed line represents the spectrum which is expected on the basis of the β-process alone while the solid line represents the fitting result including an extrapolation for the α-process based on higher temperature data.

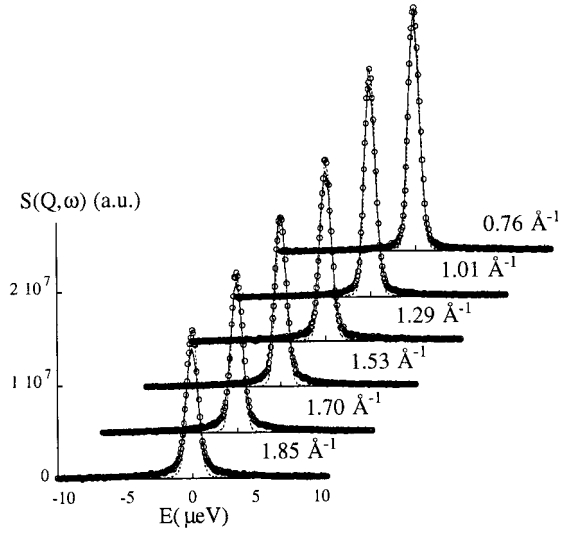

Figure 3. Q-dependence of the quasielastic spectra at 270 K. Dashed lines show the instrumental resolution (2 K spectra) for comparison and solid lines fits to eq 17.

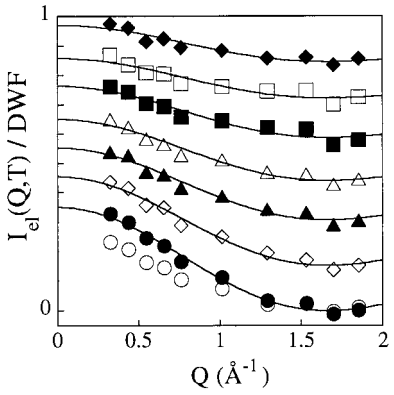

Figure 4. Q-dependence of the elastic intensity (corrected for the Debye−Waller factor and multiple scattering effects) at different temperatures: 220 K (◆); 230 K (□); 240 K (■); 250 K (△); 260 K (▲); 270 K (◇); 280 K (●). For comparison, (○) shows the same 280 K data without multiple scattering corrections. The ordinate scale shown corresponds to the 220 K data. For the rest of the temperatures the origin has been shifted for clarity (the ticks in the left axis show the corresponding "1"). Solid lines are fits to eq 11 with $d = 2.7$ Å.

Figure 3 displays selected Q-dependent spectra taken at 270 K. Again for comparison the resolution function is included in each spectrum as a dashed line. We realize that at small Q the spectra basically coincide with the resolution—no quasielastic broadening occurs—while at larger Q a clear quasielastic foot emerges which becomes more pronounced the larger Q becomes. The observation again is in qualitative agreement with the theoretical expectations outlined in section II.

Finally Figure 4 presents selected results from the temperature-dependent measurements on the elastic intensity, the so-called elastic window scan. The data were corrected for the Debye−Waller factor according to eqs 14 and 15 and for multiple scattering. For the highest temperature at 280 K, the amount of this multiple scattering correction is indicated by showing the data before and after correction. Qualitatively these elastic intensities display a Q-dependence as expected from eq 11. They show a modulation with Q which becomes the more pronounced the higher the temperature gets, reflecting the diminution of the amount of quasielastic scattering falling into the elastic window.

IV.3. Data Analysis. The data analysis proceeded in an alternating evaluation of the elastic window scan and the experimental spectra. Since the elastic data are influenced by multiple scattering which depends on the presence of quasielastic scattering, a completely independent evaluation of the elastic intensities and the quasielastic spectra is not possible.

To describe the quasielastic spectra under consideration of both the relaxation function of the β-process (eq 7) and that of the α-process (eq 9), the full scattering function of eq 8 has to be calculated. This involves a convolution of a multitude of Lorentzians from the β-process with a stretched exponential describing the α-process. To facilitate this task we used a presentation of the stretched exponential in terms of single exponentials with a distribution function $g_\alpha(\ln \tau_\alpha)$ chosen for $\beta = 0.55$.[23] The full width at half-maximum of this distribution function is 1.97 decades.

Then in ω-space both processes are formulated in terms of distributions of Lorentzians, the convolution of which can be easily performed, revealing again Lorentzians with line widths given by the sum of the corresponding widths from the convoluted pair. Thus following eq 8 the scattering function becomes

$$S(Q,\omega) = \frac{1}{2\pi}\exp\left(-\frac{\langle u^2\rangle}{3}Q^2\right)\left[\left(1+\frac{\sin(Qd)}{Qd}\right)\times \int g_\alpha(\ln\tau_\alpha)\frac{\tau_\alpha^{-1}}{\tau_\alpha^{-2}+\omega^2}\mathrm{d}(\ln\tau_\alpha) + \left(1-\frac{\sin(Qd)}{Qd}\right)\times \int g_\alpha(\ln\tau_\alpha)g_\beta(\ln\tau_\beta)\frac{(\tau_\alpha^{-1}+2\tau_\beta^{-1})}{(\tau_\alpha^{-1}+2\tau_\beta^{-1})^2+\omega^2}\times \mathrm{d}(\ln\tau_\alpha)\mathrm{d}(\ln\tau_\beta)\right] \quad (17)$$

The Q and temperature dependence of the α-relaxation were taken from the NSE experiment (eq 16). Quasielastic incoherent spectra taken in the high-temperature regime, where the α-process dominates, show, as in the case of polybutadiene,[24] that the incoherent relaxation rates are about 1 order of magnitude faster than the corresponding relaxation rates from coherent scattering.[25] An appropriate adjustment of the prefactor has been performed. Thereafter, the parameters for the α-process concerning time scale, stretching exponent ($\beta = 0.55$) and Q dependence were kept fixed. We note that the influence of the α-relaxation in the chosen temperature window is minor, and small errors in the chosen parameters would not affect our results.

The β-process was described in terms of the dielectric distribution function (eq 1) varying only the prefactor or time scale τ_0^β (eq 5) and naturally also the jump distance d. We note that for precise data evaluation an a priori knowledge of the Debye−Waller factor is very helpful, because the overall intensity correlates with the general time scale. The fit to the data was performed using the data evaluation program TOFSYS[26] which by inclusion of an adapted DISCUS subroutine[27] also allows for multiple scattering corrections.

The time scale τ_0^β and the jump distance d resulting from these fits were then used to perform the necessary multiple scattering corrections for the proper evaluation of the elastic window scan. For this purpose the Monte Carlo program DISCUS[27] was employed which, on the basis of the actual scattering function, calculates the angle and energy transfer dependent neutron fluxes for single, double, and higher order scattering. The correction for the elastic channel is then given by the ratio $R = J_1/(\sum_i J_i)$, where J_i denotes the elastically scattered neutron flux due to single ($i = 1$) and multiple scattering ($i = 2, ...$) into the direction of a given analyzer. This correction has to be performed both for the 2 K reference experiment and for each actual temperature. At 2 K the R factor is angular independent and amounts to 0.83. At higher temperatures, angle-dependent correction factors evolve which decrease with increasing scattering angle and have a larger angular breadth with increasing temperature. Figure 4 displays the maximum correction which was evaluated for 280 K. Since the R factors are closer to 1 for low Q and decrease to about the low-temperature value at higher Q, the correction [$R(T)/R(2\mathrm{K})$, $R(2\mathrm{K}) = 0.83$] is largest in the small Q regime.

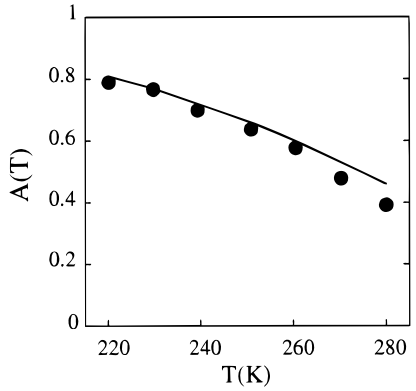

Figure 5. Temperature dependence of the quasielastic contribution factor to the elastic intensity obtained from the fits of the measured elastic intensity to eq 11 (dots). The calculated theoretical values are represented by the line.

Table 1. Quasielastic Contribution to the Measured Elastic Intensity Obtained from the Fits of the Experimental Elastic Intensity to eq 11 (A_{fit}) and that Calculated from eq 13 (A_{cal})

T (K)	$A_{fit}(T)$	$A_{cal}(T)$
280	0.39	0.46
270	0.48	0.53
260	0.58	0.60
250	0.64	0.66
240	0.70	0.72
230	0.77	0.77
220	0.79	0.81

These corrected data were fitted with the effective EISF following eq 11. Such fits reveal the jump distance and the factor $A(T)$ describing the contribution from the quasielastic spectra. A joint fit of the data at all temperatures considered revealed $d = 2.7 \pm 0.1$ Å. The corresponding to theoretical curves for the effective EISF are displayed as solid lines in Figure 4. The resulting quasielastic contribution factors $A(T)$ are listed in Table 1 and are displayed in Figure 5.

In a second step, keeping $d = 2.7$ Å fixed, we went back to the fit of the quasielastic spectra and iterated the time scale of the β-process, τ_0^β, including multiple scattering corrections again using DISCUS. Convergence was generally achieved after three steps. The modifications for τ_0^β resulting from this procedure did not affect the corrections for the EISF.

The final outcome of this fit is presented by the solid lines in Figures 2 and 3 which describe the spectra

generally very well. The slight discrepancies in the regions of the peak at high Q may result from the weighting procedure employed for the mean square deviations between the theoretical scattering function including all multiple scattering events and the data. We weighted with pseudostatistical errors given by the square root of the count rate. Therefore the wings of the spectra are strongly emphasized. A small remaining sample-dependent background could have caused the observed deviations. A linear weighting on the other hand always overestimates the importance of the peak region and is not appropriate if we are interested in the quasielastic wings.

Within the experimental error the time scale τ_o^β, which besides a common intensity factor for all spectra was the only adjustable parameter in the fits of the quasielastic spectra, turned out to be independent of temperature and was determined to $\tau_o^\beta = 4 \times 10^{-14}$ s, i.e., about 4 times shorter than the corresponding value of 1.5×10^{-13} s from the dielectric measurements. Fits also allowing the variation of the jump distance d led again to $d = 2.7$ Å as determined from the EISF measurements. The factor of 4 found between the time scale of the β process obtained respectively by dielectric and neutron techniques can easily be accepted taking into account the different experimental techniques which relate to different correlation functions. However, it is worthy of remark that this simple argument does not work in the case of polybutadiene, where a still not understood factor of about 2 orders of magnitude was found.[19]

While the quasielastic spectra were only taken in a narrow temperature window, the elastic window scan covered a much larger range. Furthermore, we are confronted with a broad distribution of jump rates where, even at low temperatures, processes exist which still give rise to quasielastic broadening within the experimental observation window. To perform a consistency check and to test the dielectric distribution function over a larger temperature range, we used eq 13 and calculated theoretical quasielastic contribution factors $A(T)$ to the elastic intensity. These factors $A(T)$ are sensitive both to the chosen time scale τ_o^β as well as to the breadth of the distribution. The resulting values are listed in Table 1. Figure 5 compares these theoretical factors $A(T)$ with results from the fit of the elastic data (Figure 4). We find astonishingly good agreement between experiment and theoretical expectation. We note that the deviations observed for $T = 270$ K and $T = 280$ K can be easily understood. From the extrapolation of the α-process we expect some traces to be seen in the spectra at 270 and 280 K which are not accounted for in eq 13. Thus we can state that in terms of the dielectric β−process found for PIB, the quasielastic incoherent neutron spectra as well as the elastic window measurements can be described very consistently, revealing both the time and the length scales of the protonic motion associated with this process.

V. Discussion

V.1. Comparison with Results from Spectroscopic Techniques. Figure 6 positions our results from the IQENS study into the frame of the existing body of data.[6,15] The peak relaxation rates for the β-process relating to $\tau_\beta(E_o)^{-1}$ which were obtained from the direct fit of the quasielastic spectra, are shown as full squares. The full solid line through these points

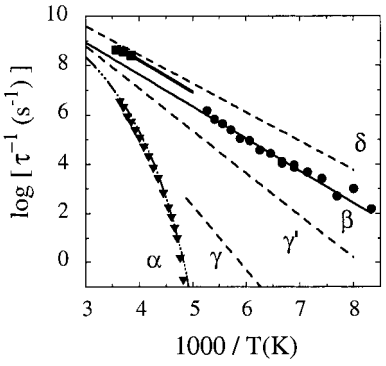

Figure 6. Arrhenius plot of the characteristic frequencies (corresponding to the maximum of the dielectric loss) of the α- (▼) and β-relaxation (●). The solid line represents a fit with an Arrhenius law. Dashed−dotted and dashed lines are the temperature laws shown in ref 6 for the α-relaxation and the different secondary relaxations, respectively. The squares correspond to the characteristic rates of the β-process obtained from the quasielastic IN16 spectra and the thick solid line shows those deduced from the analysis of the elastic intensities.

extending to lower temperatures presents what could be inferred from the elastic window scan [$A(T)$ parameter, eq 13]. Furthermore, Figure 6 includes the δ-process, the newly discovered dielectric β-process, and the hypothetical γ- and γ'-relaxations as well as the dielectric α-process. We realize that the neutron-based relaxation rates within experimental error hit those for the δ-process.

This δ-relaxation had been studied by spectroscopic techniques such as NMR[11] and ESR[6] and was assigned by Slichter[11] to originate undoubtedly from a methyl-group rotation. We had already remarked earlier[15] that the dielectric process which we had termed "β" had practically the same activation energy as the δ-process. But since methyl-group rotation is not dielectrically active, the idea that the dielectric β- and the δ-process could be identical was not considered. Now with the quasielastic neutron data at hand, we are in the position to revise the earlier assignment of the δ-process as due to methyl-group rotations.

(i) The IQENS data can be consistently described in terms of the activation energy and the distribution parameters of the dielectric β-process which cannot be due to a methyl group rotation.

(ii) The IQENS data reveal a jump distance or more generally a spatial extent of the associated motion of 2.7 Å by far too large for a methyl reorientation.

(iii) The quoted coherent quasielastic neutron spectra taken at the NSE spectrometer contain signatures of the β-process. A 3-fold methyl-group jump would be invisible in coherent scattering (see below).

(iv) Finally, Figure 7 presents the comparison of the EISF data at two selected temperatures (260, 280 K) with the EISF following from a methyl-group rotation.[28] There we have

$$I_{el}(Q,\omega \approx 0) = \frac{3}{4}\left[\frac{1}{3}\left(1 + 2\frac{\sin Qr_{HH}}{Qr_{HH}}\right) + A\frac{2}{3}\left(1 - \frac{\sin Qr_{HH}}{Qr_{HH}}\right)\right] + \frac{1}{4} \quad (18)$$

where $r_{HH} = 1.78$ Å is the H−H distance and factors $^3/_4$ and $^1/_4$ account for the relative amount of protons positioned within a methyl group or at the CH_2 unit,

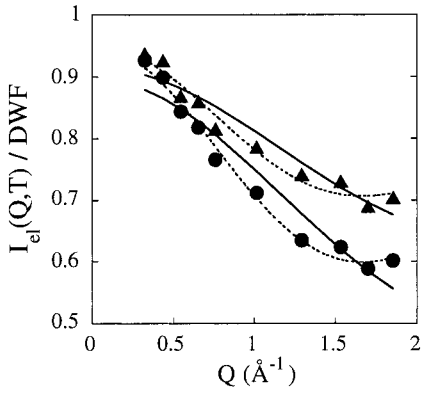

Figure 7. Comparison between the descriptions of the elastic intensity at 260 K (▲) and 280 K (●) in terms of the EISF corresponding to a methyl-group rotation (solid lines) and to a two-site jump (dashed lines).

respectively. Figure 7 also includes the results with the two-site EISF explained in Section IV (dashed lines). It is evident from Figure 7 that while the two-site EISF with $d = 2.7$ Å is in very good agreement with the data, the methyl group EISF deviates systematically.

Thus, since on one hand the neutron data lead to identical time scales and temperature dependencies as the δ-process and, on the other hand, they agree quantitatively with the dielectric distribution parameters including the activation energy, we conclude that both processes are identical even though the dielectric β-process is a factor of 4 slower. Then the δ-process cannot be understood in terms of only a methyl-group rotation as proposed by NMR but must be related to a conformational rearrangement. This explains its visibility in dielectric spectroscopy and the large motional amplitude derived from the IQENS experiment. Finally a conformational process also makes plausible the observation of this process in Brillouin scattering as reported by Patterson.[29] It is hard to understand how methyl-group reorientation should couple to sound waves.

V.2. Relation to Results from Coherent Quasielastic Neutron Scattering. As it has already been mentioned, from coherent quasielastic neutron scattering undertaken on a fully deuterated PIB sample, a local jump process evolved apparently exhibiting a motional amplitude of $d_{coh} \cong 0.9$ Å. The distribution parameters as well as the time scale of this process were compatible with the dielectric result. In contrast, in our present IQENS data the same process is seen in terms of its self-correlation function extending over a much larger spatial extent ($d = 2.7$ Å). Going back to the quasielastic coherent spectra it turns out, that such a large jump distance is clearly incompatible with the NSE data. Thus, we may ask: how can the same process appear on different length scales in the self- and the pair-correlation functions, respectively?

Qualitatively we may consider rotational motion of molecular parts around an axis of local symmetry. Then, while for the self-correlation function the motional extent is given by twice the motional radius, for the pair correlation function which is sensitive to density fluctuations, due to the internal symmetry the fluctuations are reduced. Consider, e.g., a molecule with 3-fold symmetry to rotate around the 3-fold axis. Then, all fluctuations seen in the selfmotion are reduced by modulo ($2\pi/3$) for the pair correlation.

To be more quantitative, the self-correlation function, being the conditional probability to find a particle at time t at position $\underline{r}$ if the same particle was at time $t = 0$ at position $\underline{r} = 0$, traces the complete motion of a tagged particle. On the other hand, coherent QENS is sensitive to the change of configurations of atoms.[19] E.g., for a methyl group, a 3-fold jump leads to identical atom positions before and after the jump—there would be no quasielastic coherent neutron scattering.

Now let us demonstrate the difference between coherent and incoherent quasielastic neutron scattering for rotational motions on an example. We consider rotational diffusion of an object with N-fold internal symmetry on a circle.[28] If $P(\phi,\phi_o,t)$ is the probability to find a certain atom at the angle ϕ at time t, if it was at ϕ_o for $t = 0$, then this probability follows the diffusion equation

$$D_r \frac{\partial^2 P(\phi,\phi_o,t)}{\partial \phi^2} = \frac{\partial}{\partial t} P(\phi,\phi_o,t) \tag{19}$$

with the solution

$$P(\phi,\phi_o,t) = \frac{1}{2\pi} \sum_{n=-\infty}^{+\infty} \exp[\ln(\phi - \phi_o)] \exp(-D_r n^2 t) \tag{20}$$

where D_r is the rotational diffusion coefficient. Coherent quasielastic scattering measures the interference pattern between the initial and the final configuration of atoms. Thus we have to take the scattering amplitudes and let them interfere for an object with N-fold symmetry. To make it simple we take N atoms equally spaced at an angular distance of $2\pi/N$ on a circle of radius r. For the amplitudes in the initial and final states we have

$$A_i(\underline{Q},\phi_o) = \sum_i e^{i\underline{Q}\underline{r}_i(\phi_o)}; \quad A_f(\underline{Q},\phi) = \sum_i e^{i\underline{Q}\underline{r}_i(\phi)} \tag{21}$$

with $\underline{Q}\,\underline{r}_i = Qr \sin\vartheta \cos(\phi_o - \varphi + (2\pi/N)\, i)$.

ϑ and φ are the spherical coordinates of the $\underline{Q}$ vector. The intermediate dynamic structure factor becomes

$$S(\underline{Q},t) = \frac{1}{N}\frac{1}{2\pi}\int_0^{2\pi} d\phi_o \int_0^{2\pi} d\phi\, A_f^*(\underline{Q},\phi) A_i(\underline{Q},\phi_o) P(\phi,\phi_o,t) \tag{22}$$

With the usual expansions of the exponentials into harmonics and converting into ω-space, the resulting coherent dynamic structure factor is obtained:

$$S(\underline{Q},\omega) = N\, J_o^2(Qr \sin\vartheta) + \frac{2}{N}\sum_{n=1}^{\infty}\sum_{l,s=1}^{\infty} J_n^2(Q\, r \sin\vartheta) \cos\left[\frac{2\pi n}{N}(l-s)\right] \frac{D_r\, n^2}{D_r\, n^2 + \omega^2} \tag{23}$$

Here $J_n(x)$ are Bessel functions. The self-correlation functions evolve for $N = 1$. The resulting weight functions or form factors for the quasielastic contributions are very instructive and are displayed for $N = 3$ in Figure 8. Figure 8a shows the coherent form factors while Figure 8b presents the corresponding form factors for the self-correlation function. In the case of the pair correlation function the cosine factors in eq 23 eliminate the first and second quasielastic term—they correspond

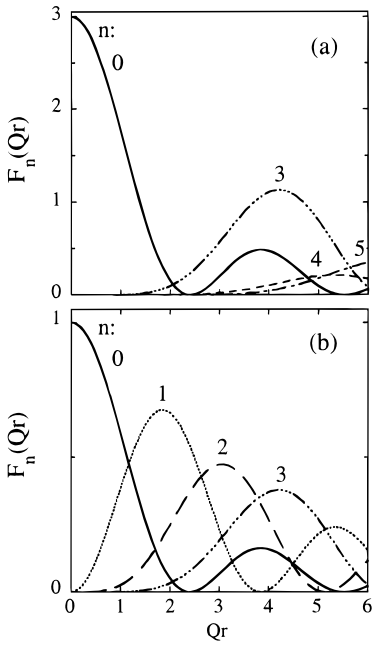

Figure 8. Form factors of the quasielastic contributions to the (a) pair- and (b) self-correlation function of a 3-fold object rotating around its 3-fold axis. Different lines correspond to different orders n (in part a, the function is identical to 0 for $n = 1$ and 2).

to angular displacements larger than $2\pi/3$—and the first quasielastic line corresponds to motions with the symmetry constraint modulo ($2\pi/3$). The first maximum weight is achieved for $Qr = 4.2$.

Now we turn to the self-correlation function. There all cosine factors are 1 and the whole series of eq 23 contributes (Figure 8b). In this case we reach the first maximum of a quasielastic form factor (from J_1^2) at $Qr = 1.8$. The positions of maximal form factor are generally identified with the length scale. Consequently a shift of the first observable maximum from 1.8 to 4.2 due to coherency effects appears as a reduction of length scale by 2.33. Thus, for our example of a 3-fold object rotating around its 3-fold axis, a length scale of 2.7 Å in the self-correlation function would appear in coherent quasielastic scattering as a length of 1.16 Å, if coherency effects are not taken into account.

This example is not a final word on the observed discrepancy between the length scales observed by coherent and incoherent quasielastic scattering on the same process, but it indicates a possible solution. Conformational dynamics locally are to a large extent rotational motions; again locally polymers are often tetrahedrally coordinated, leading to local 3-fold symmetries or at least something close to it. Our observation of a large discrepancy between the length scales from the pair and the self-correlation functions can be taken as a signature for a rotational motion, although the particular mechanism cannot be established only from these results. On the other hand, one can also consider the possibility of a strong coupling between the rotation of the two methyl groups linked to the same carbon and the local backbone motions giving rise to the dielectrically active β-process. This possibility would be suggested by the high value of the frequency of the methyl-group torsional librations ($\approx$ 40 meV) measured by inelastic neutron scattering in PIB[30] implying a very stiff methyl-group rotational potential. In this kind of scenario, it could be assumed that backbone motion leading to conformational changes also induces, e.g., by steric effects, methyl-group rotation. Such a coupling mechanism could bring together the NMR observation of a methyl-group rotation, the dielectric results which are only sensitive to dipole motions, the incoherent neutron data which see the total H-displacement and the coherent data, where methyl-group rotations are not or only weakly visible. However, it is clear that a detailed explanation needs extended computer simulation including the calculation of the incoherent scattering function and the dynamic structure factor on the basis of a realistic model for polyisobutylene.

VI. Conclusions

By quasielastic incoherent neutron scattering we have investigated the local dynamics of PIB in a temperature region, where the α-process is not (or only weakly) contributing to the neutron spectra. We have exploited the capabilities of IQENS in studying both the quasielastic spectra as well as the elastic incoherent structure factor. The elastic studies, thereby, had a much wider temperature breadth.

The data were evaluated on the basis of a distribution of jump rates determined earlier by dielectric spectroscopy. Data corrections included the calculation of multiple scattering effects, which, even for a sample with high transmission, influence the quasielastic data considerably in particular at smaller momentum transfers. With these data treatments a very consistent description of all available spectra and elastic data could be accomplished. We note that the good agreement between the theoretically calculated and the measured elastic data serves as a severe test of the jump rate distribution taken from the dielectric spectra.

Our experimental results reveal the protonic motion which underlies the dielectric β-process and characterize this motion as locally restricted with a relatively large motional amplitude of 2.7 Å. Furthermore the experiment strongly suggests that the dielectric β-process and the so-called δ-process are identical qualifying, thereby, the old assignment of the δ-process as only due to methyl-group rotations as incorrect.

Finally we have discussed the paradox that measurements of the pair- and self-correlation functions for the same relaxation process in PIB reveal significantly different length scales. We have shown that for rotational motions around an axis of internal symmetry, if coherency effects are not considered, the interpretation of quasielastic coherent scattering will lead to seemingly shorter length scales than those revealed from a measurement of the self-correlation function.

Acknowledgment. We acknowledge partial support by the Acciones Integradas Spain-Germany (Contract: AI 95-09). Financial support from the projects MEC PB94-0468, G.V. PI95/005, and UPV 206.215-EC245/96 is acknowledged by J.C. A.A. also acknowledges the Grant of the Basque Government, and D.R. and J.C. acknowledge the BBV-Foundation (programa Cátedra). We are thankful to L. Willner for the sample characterization.

References and Notes

(1) Ferry, J. D. In *Viscoelastic Properties of Polymers*; John Wiley & Sons: New York, 1970.
(2) Fitzgerald, E. R.; Grandine, L. D., Jr.; Ferry, J. D. *J. Appl. Phys.* **1953**, *24*, 650. Ferry, J. D.; Grandine, L. D., Jr.; Fitzgerald, E. R. *J. Appl. Phys.* **1953**, *24*, 911.

(3) Philippoff, W. *J. Appl. Phys.* **1953**, *24*, 685.
(4) Tobolsky, A. V.; Catsiff, E. *J. Polym. Sci.* **1956**, *19*, 111.
(5) Frick, B.; Richter, D. *Phys. Rev. B* **1993**, *47*, 14795.
(6) Törmälä, P. *J. Macromol. Sci.—Rev. Macromol. Chem. C* **1979**, *17*, 297.
(7) Plazek, D. J.; Zheng, X. D.; Ngai, K. L. *Macromolecules* **1992**, *25*, 4920.
(8) Ngai, K. L.; Plazek, D. J.; Bero, C. A. *Macromolecules* **1993**, *26*, 1065.
(9) Plazek, D. J.; Chay, I.-C.; Ngai, K. L.; Roland, C. M. *Macromolecules* **1995**, *28*, 6432.
(10) Suter, U. W.; Saiz, E.; Flory, P. J. *Macromolecules* **1983**, *16*, 1317.
(11) Slichter, W. P. *J. Polym. Sci.: Part C* **1966**, *14*, 33.
(12) Dejean de la Batie, R.; Lauprêtre, F.; Monnerie. L. *Macromolecules* **1989**, *22*, 2617.
(13) McCrum, N. G.; Read, B. E.; Williams, G. In *Anelastic and Dielectric Effects in Polymeric Solids*; Wiley: London, 1967; p 389.
(14) Stoll, B.; Pechhold, W.; Blasenbrey, S. *Kolloid-Z.* **1972**, *250*, 1111.
(15) Richter, D.; Arbe, A.; Colmenero, J.; Monkenbusch, M.; Farago, B.; Faust, R. *Macromolecules* **1998**, *31*, 1133.
(16) Johari, G. P.; Goldstein, M. *J. Chem. Phys.* **1970**, *53*, 2372.
(17) Springer, T. In *Quasielastic Neutron Scattering for the Investigation of Diffusive Motions in Solids and Liquids*; Springer Tracts in Modern Physics; Springer: Berlin, 1972; p 64.
(18) Arbe, A.; Buchenau, U.; Willner, L.; Richter, D.; Farago, B.; Colmenero, J. *Phys. Rev. Lett.* **1996**, *76*, 1872.
(19) Arbe, A.; Richter, D.; Colmenero, J.; Farago, B. *Phys. Rev. E.* **1996**, *54*, 3853.
(20) Colmenero, J.; Alegría, A.; Arbe, A.; Frick, B. *Phys. Rev. Lett.* **1992**, *69*, 478.
(21) Zorn, R.; Arbe, A.; Colmenero, J.; Frick, B.; Richter, D.; Buchenau, U. *Phys. Rev. E* **1995**, *52*, 781.
(22) Alefeld, B.; Birr, M.; Heidemann, A. *Naturwissenschaften* **1969**, *56*, 410.
(23) Gómez, D.; Alegría, A.; Colmenero, J. To be published.
(24) Arbe, A.; et al. To be published.
(25) Arbe, A.; et al. To be published.
(26) TOFSYS is a multipurpose program for data treatment and nonlinear fitting on spectra obtained from time-of-flight or backscattering instruments, developed (Monkenbusch, M.; Buchenau, U.; Prager, M.; Schaetzler, L.) and used in the neutron scattering groups in Jülich.
(27) Johnson, M. W. *DISCUS: A Computer Program for the Calculation of Multiple Scattering Effects in Inelastic Neutron Scattering Experiments*. HARWELL HL74/1054(C13).
(28) See, e.g.: Bee, M. *Quasielastic Neutron Scattering*; Adam Hilger: Bristol, England, 1988.
(29) Patterson, G. D. *J. Polym. Sci.: Polym. Phys. Ed.* **1977**, *15*, 455.
(30) Frick, B.; Richter, D. *Phys. Rev. B* **1993**, *47*, 14795.

MA9717810